Nd and Sr isotope systematics and geochemistry of plume related early Cretaceous alkaline-mafic-ultramafic igneous complex from Jasra, Shillong Plateau, Northeastern India

RAJESH K. SRIVASTAVA* and ANUP K. SINHA

Igneous Petrology Laboratory, Department of Geology, Banaras Hindu University, Varanasi 221 005, India
(* Corresponding author: e-mail: rajeshgeolbhu@yahoo.com)

Abstract – This paper describes an early Cretaceous Jasra alkaline-mafic-ultramafic igneous complex related to Kerguelen hotspot-mantle plume system of Indian Ocean. This complex, emplaced in the Shillong plateau, consists mainly of pyroxenite, gabbro and nepheline syenite and is closely associated to the Barapani-Tyrsad shear zone, Kopali faults, and Um Ngot lineaments. Pyroxenite and gabbro occur as separate plutons, whereas nepheline syenites occur either in the form of small dikes in pyroxenites or as differentiated bodies in the gabbros. A few mafic dikes, contemporaneous to gabbro, cut pyroxenite and granite bodies. Mineral compositions classify the pyroxenites into pyroxenite and alkali pyroxenite and the gabbros into essexite and olivine gabbro. Chemical and normative compositions of mafic-ultramafic rocks also show their alkaline nature. Nepheline syenite samples are miaskitic in character (agpaitic index < 1) suggesting involvement of CO_2 related phase in their genesis. Chemical data do not support any simple genetic relationship between the different rock units of the complex. Field-data also support this conclusion and suggest that they have different genetic histories. Major element based discrimination function diagrams suggest ocean-island basalt (OIB) affinity of Jasra samples. OIB nature of these samples is further corroborated by their radiogenic isotopic compositions

Sr and Nd isotopic compositions ($^{87}Sr/^{86}Sr_{initial}$ between 0.706523 and 0.708891 and $^{143}Nd/^{144}Nd_{initial}$ between 0.512258 and 0.512464) suggest that these rocks were derived from a mixing of mantle components like HIMU (mantle with high U/Pb ratio) and EM (enriched mantle) components, which show close isotopic composition similar to FOZO. Lherzolite

mantle was metasomatized into an alkaline wehrlite by CO_2, released by low-degree melting of a carbonated mantle peridotite. Melting of such a metasomatized mantle source may produce ultrabasic alkaline silicate magma, from which the different rock units of the Jasra complex were crystallized. The geological, geochemical, geochronological, and isotopic data also suggest a spatial and temporal association with the Kerguelen plume activity.

Keywords: Alkaline-ultramafic-mafic complex, Radiogenic isotopes, Geochemistry, Jasra, Shillong plateau, Kerguelen plume, CO_2-Metasomatism.

INTRODUCTION

A large igneous province (LIP), located in the southern Indian Ocean, covers a massive region consisting of Kerguelen plateau, Broken Ridge, Bunbury, and northeastern India (see Fig. 1), which represents the volcanic outpouring from a Kerguelen hotspot-mantle plume system since ~132 Ma (Coffin et al., 2002; Kent et al., 1997, 2002). The Kerguelen LIP also marks the break-up of India and Australia and it is usually believed to be related to hotspot activity over a period of up to 130 Ma (Frey et al., 2000; Kent et al., 2002).

An association between alkaline magmatism and mantle plumes has frequently been proposed (Franz et al., 1999; Bell, 2001, 2002). This is more realistic if alkaline magmatism is found associated with carbonatite. There are some other models, such as rift-setting or subduction related magmatism (Luhr, 1997; Sheth et al., 2000; Verma, 2006), which may also explain genesis of alkaline magmas (Wilson, 1989). Alkaline magma may be generated by low-degree melting of an enriched mantle source or by pronounced differentiation of a mafic magma or even by crustal contamination of mantle derived magma; volatile contents and mantle mineralogy also affect magma compositions (Mahoney et al., 1985; Wilson, 1989; Winter, 2001). It is also observed that the latest phases of continental flood basalts (CFB) are spatially and temporally associated with alkaline and carbonatite magmatism (Heaman et al., 2002; Bell,

2001, 2002). One reason for relating such alkaline magmatism to plume activity is the isotopic similarity between these rocks and Ocean-island basalts (OIB). To establish such relationships, radiogenic isotope data are helpful to identify components such as depleted MORB mantle (DMM), mantle with high U/Pb ratio (HIMU), enriched mantle with high Rb/Sr, low U/Pb and Sm/Nd ratios (EM-I), enriched mantle with high Rb/Sr and U/Pb and low Sm/Nd ratios (EM-II), and focal zone mantle component (FOZO) (Zindler and Hart, 1986; Hart, 1988; Hart et al., 1992; Bell, 2002).

The Shillong plateau of NE India underwent early Cretaceous basic and alkaline carbonatite activity. Many earlier workers proposed spatial and temporal association of these magmatism with a plume currently beneath Kerguelen (Storey et al., 1992; Ray et al., 1999; Kent et al., 1997, 2002; Srivastava et al., 2005). It is suggested that Kerguelen hotspot was situated very close to the eastern Indian margin during 100-120 Ma (cf. Fig. 5 of Coffin et al., 2002; Fig. 4 of Kent et al., 2002) and responsible for the Rajmahal basalts exposed over the Gondwana Supergroup and Sylhet basalts and alkaline-carbonatite magmatism of the Shillong plateau. The Jasra alkaline-mafic-ultramafic complex (Fig. 2a) selected for this study is situated in the Karbi Anglong district of Assam at the eastern part of Shillong plateau. Mamallan et al. (1994) were the first to document this complex, and Srivastava and Sinha (2004) subsequently presented a detailed petrological and whole rock geochemical data for these rocks. Heaman et al. (2002) dated this complex applying the U-Pb method to zircon and baddeleyite, which placed it at 105.2±0.5 Ma, roughly contemporaneous with other nearby complexes (Table 1). Because there are no isotopic data available to discuss the petrogenesis of different rock types associated with the Jasra complex, this paper presents the first radiogenic isotopic data from the Jasra alkaline-mafic-ultramafic complex. Using other petrological and geochemical data we attempt to evaluate the nature of the source, whether derived from mantle components or has some other genetic history, for the genesis of this complex.

GEOLOGICAL SETTING

The Shillong plateau, NE India, underwent extensive magmatic activity that ranged from granitic to alkaline composition. Most of the rocks were emplaced into the Proterozoic Shillong Group, consisting of orthoquartzite and phyllite, within the basement Archaean gneissic complex (Desikachar, 1974; Mazumdar, 1976). In addition, Neoproterozoic granite plutons, small bodies of metamorphosed mafic igneous rocks, many exposures of early Cretaceous basaltic flows (Sylhet traps), and alkaline-(carbonatite)-mafic-ultramafic complexes are emplaced in the Shillong Group (Fig. 2a; Mazumdar, 1976; Ghose et al., 1994; Kumar et al., 1996; Das Gupta and Biswas, 2000).

The Shillong plateau (Fig. 2a) is a rectangular-shaped uplifted horst-like feature, bounded all sides by deep fault systems (Evans, 1964; Desikachar, 1974; Nandy, 1980; Gupta and Sen, 1988; Golani, 1991). The Jasra alkaline-mafic-ultramafic igneous complex is situated within the prominent fracture system of the Barapani-Tyrsad Shear zone, Kopili fault, and Um Ngot lineaments (Fig. 2a). There is no geological or geophysical feature observed or reported from the Shillong plateau to indicate extensional or subduction tectonics (Evans, 1964; Desikachar, 1974; Nandy, 1980; Gupta and Sen, 1988; Das Gupta and Biswas, 2000; Kayal et al., 2006). It is believed that the set of N-S trending faults and lineaments of the Shillong plateau were developed initially during the late Jurassic – early Cretaceous times and closely associated to the early Cretaceous igneous intrusions, including alkaline and carbonatite complexes (Gupta and Sen, 1988).

Mamallan et al. (1994) and Srivastava and Sinha (2004) have described the geology of the Jasra alkaline-mafic-ultramafic igneous complex. This complex consists of pyroxenite, gabbro, a few mafic dikes and nepheline syenite (Fig. 2b). Coarse-grained pyroxenite and gabbro form separate pluton, although it is difficult to observe any field relationship between the pyroxenite

and gabbro plutons. Srivastava and Sinha (2004) reported that a few mafic dikes, contemporaneous with the gabbro plutons, sharply cut the pyroxenites as well as the granitic rocks, but not the gabbroic plutons. This relationship suggests that the mafic gabbro and dikes are younger than the pyroxenite. Small dikes and dikelets of nepheline syenite cut all rock types, and form the youngest unit of this complex. In places, a few thin sections exhibit accumulation of nepheline and alkali pyroxene grains and show an ijolitic nature for these rocks. This is important because ijolite-nephelinite is thought to be often associated with the alkaline-carbonatite magmatism (Le Bas, 1987, 1989). Calcite grains are also observed in the pyroxenite samples, but no separate exposure of ijolite or carbonatite has yet been found.

Srivastava and Sinha (2004) have already described, in detail, the petrography of major rock types associated with the Jasra complex (Table 2). Mineral compositions along with textures, based on study of about seventy samples, classify the pyroxenites as clinopyroxenite, olivine clinopyroxenite and alkali pyroxenite, whereas gabbro samples show variations from monzogabbro (essexite) to olivine gabbro. Syenite samples contain nepheline.

ANALYTICAL TECHNIQUES

Whole rock major elements (for sixteen samples) and trace (+ rare-earth) elements (for ten samples) were analysed at the Activation Laboratories Ltd., Ancaster, Canada. An ICP-OES (Model: Thermo-JarretAsh ENVIRO II) was used to analyse major elements, whereas an ICP-MS (Model: Perkin Elmer Sciex ELAN 6000) was used to determine trace element concentrations. Several international geochemical reference material samples (STM1, MRG1, DNC1, SY3, and W2) were run along with Jasra samples in order to assess the accuracy of our result. Precision and accuracy were approximately 5% and 5-10%, when reported at 100X the detection limit, for major oxides and trace/rare-earth elements, respectively. Whole rock major oxide and CIPW normative compositions are presented in Table 3. CIPW norms, rock-types,

and Mg# for all samples were automatically computed using the SINCLAS Computer Program (Verma et al., 2002). In the "Middlemost option of this program the iron-ratio used for CIPW norm calculation is taken from Middlemost (1989). Table 4 presents whole rock trace and rare-earth element compositions. Locations of the samples analysed are marked on the geological map (Fig. 2b).

Radiogenic isotopic compositions were measured at the Research Center for Mineral Exploration (RCMRE), Beijing, PR China. A Thermo Finnigan MAT 262 multi-collector mass spectrometer was used for the radiogenic isotope (Sm-Nd and Rb-Sr) analyses. International standards La Jolla and BCR-1 were used for the Nd isotope analyses and NBS987 and NBS607 were used for the Sr isotope analyses. The two standard deviation uncertainties on the measured $^{87}Sr/^{86}Sr$ and $^{143}Nd/^{144}Nd$ isotope ratios are considered to be better than ±0.002% and ±0.001% respectively. Analyzed isotope data are presented in Table 5. Initial isotopic ratios were calculated assuming an emplacement age of 105 Ma for the Jasra complex dated by a precise U-Pb method using zircon/baddeleyite from a differentiated gabbro, which placed it at 105.2±0.5 Ma (Heaman et al., 2002). We do not have age for other units of the complex but it is presumed that older and younger phases of this complex may have been emplaced at an interval of ~5 Ma. Initial isotopic ratios were also calculated assuming 100 Ma and 110 Ma and found to be within the analytical error bars.

GEOCHEMISTRY

Whole rock geochemistry

Classification based on the total alkali and silica contents (TAS) is presented in Table 3. This classification, based on IUGS recommendations (Le Maitre, 2002), was obtained with the help of the SINCLAS computer program (Verma et al., 2002). Pyroxenite samples were classified as melanephelinite foidite to melanephelinite basanite. The gabbroic samples indicate

melanephelinite tephrite, potassic trachybasalt, alkali basalt, and melanephelinite basanite compositions. Syenite samples are tephriphonolite in nature. Thus, it is concluded that most samples show melanephelinitic compositions. CIPW normative compositions (Table 4) also corroborate the alkaline nature of these rocks. All of the pyroxenite samples contain alkaline normative minerals such as nepheline (*ne*), leucite (*lc*), and dicalcium silicate (*cs*). Similarly, gabbro samples have orthoclase (*or*), albite (*ab*), and nepheline (*ne*) in their normative compositions. The agpaitic indices [= $(Na_2O+K_2O)/Al_2O_3$ ratio or $(Na+K)/Al$] for both the nepheline syenite samples are < 1, suggesting a miaskitic affinity (Heinrich, 1966; Bates and Jackson, 1980). This is an important feature; miaskitic nepheline syenites have a very close relationship with carbonatite magmatism; but it is also realized that more analyses of nepheline syenite samples is required for any strengthen conclusion. Such syenitic rock is also found to be enriched in CO_2 leading to crystallization of cancrinite and calcite (Heinrich, 1966). High Mg number ($\cong 62$) and MgO > 6% are indicative of primary magma (Green, 1971; Luhr, 1997; Velasco-Tapia and Verma, 2001). Some samples of present study have similar Mg number and most have similar MgO contents. Other samples, including syenites, are probably differentiated products of a primary magma. Thus, we believe that studied Jasra samples are either derived from a primary magma or differentiated products of primary magma.

With reference to Harker and other variation diagrams we, in earlier paper (Srivastava and Sinha, 2004), suggested that all three major rock types do not show any co-genetic relationship with each other and probably have different genetic histories. Few new variation diagrams (not presented in Srivastava and Sinha, 2004) are shown in Figure 3. Important characteristics observed from these plots are –

(i) Pyroxenite and gabbro samples show similar chemical composition and linear trends but probably not suggesting any simple differentiation process,

(ii) This observation is more evident from the Mg# vs SiO$_2$ (Figure 3a) and Zr vs SiO$_2$ (Figure 3b) plots. On these plots all the three rock types plot separately and show different crystallization trends. More significantly at a given Zr contents different rock types have different silica contents (Figure 3b); which is difficult to explain by simple differentiation of a single batch of magma, and

(iii) One syenite sample (JS/5S), collected from the differentiated part of a gabbro, indicates differentiation; it has a high concentration of HFSE.

Thus, it is apparent that different rock types of the Jasra complex probably have different evolutionary histories.

These geochemical characteristics are further evident from the primordial-mantle normalized multi-element and chondrite normalized rare-earth element patterns for the Jasra samples (Figure 4). Multi-element plots of pyroxenite and gabbro samples show similar patterns, quite unlike those from the syenite samples. However, the rare-earth element patterns of all the samples are similar. Again, it is difficult to explain relationship between different rock types of the Jasra complex by a differentiation process; if gabbro is a differentiated product of pyroxenite, it should have higher concentrations of REE than the pyroxenite but this is not so. Multi-element pattern of one syenite sample (JS/5S) is similar to the patterns of gabbro samples, but the other sample (JS/15S) shows an entirely different pattern suggesting that both samples have different crystallization histories. Beside these characteristic HFSE patterns also illustrate no or positive Nb, Ta (with respect to K and La) and Ti (with respect to Sm and Tb) anomalies. Such geochemical characteristics clearly preclude role of crust in the genesis of Jasra samples; crustal contaminated samples should have negative Nb, Ta and Ti anomalies (Wilson, 1989; Carlson, 1991; Saunders et al., 1992; Kent, 1995; Winter, 2001). Similar geochemical characteristics are also observed for some modern ocean-island basalts (Saunders et al., 1992; Kent, 1995). This feature for Jasra samples is very clearly observed from the Figure 5 (Agrawal

et al., 2004; Verma, et al., 2006). These authors have presented a set of new discrimination function diagrams based on the major element data to interpret nature of magma type and emplacement tectonic environment. This set of plots can discriminate among island arc, continental rift, ocean-island, and mid-ocean ridge tectonic settings. On these diagrams Jasra samples proved to be of ocean-island basalt (OIB) affinity because Jasra samples show a high percentage (about 86 to 100%) plot in the OIB field in these diagrams. LREE enriched patterns are observed either in the subducted related (i.e. involvement of crustal material) magmatism or low-degree partial mantle melting or through some metasomatic process (Cullers and Graf, 1984). It is correct that samples derived from a crust-contaminated melt show LREE enriched patterns but such samples should also have negative Nb, Ta and Ti anomalies on multi-element patterns; which is different from the Jasra samples. Small degree of melting (< 10%) of mantle peridotite may show an enriched LREE pattern (Cullers and Graf, 1984). Thus, low-degree partial melting of a mantle together with metasomatic process looks more appropriate for Jasra rocks. These observed geochemical characteristics most likely preclude possibility of crustal contamination and suggest that Jasra samples are derived from a mantle derived melt of OIB affinity.

Radiogenic isotope geochemistry

$^{87}Sr/^{86}Sr_{initial}$ and $^{143}Nd/^{144}Nd_{initial}$ ratios in the Jasra samples show variation between 0.706523 to 0.708891 and 0.512258 to 0.512464, respectively. All samples have positive εSr values (+30.5 to +64.1) and negative εNd values (-0.76 to -4.78). Isotopic data of all the samples are plotted in the $^{87}Sr/^{86}Sr_{initial}$ versus $^{143}Nd/^{144}Nd_{initial}$ diagram (Fig. 6a). All samples plot close to the enriched mantle field. The pyroxenite samples have the lowest $^{87}Sr/^{86}Sr_{initial}$ ratios and the gabbro sample has the highest $^{143}Nd/^{144}Nd_{initial}$ ratios, whereas $^{143}Nd/^{144}Nd_{initial}$ ratios show very

limited variation. The high $^{87}Sr/^{86}Sr$ values observed in these samples are probably the result of metasomatism by fluids/melts with an enriched mantle signature.

Zindler and Hart (1986) and Hart (1988) defined different mantle reservoirs on the basis of their isotopic taxonomy and proposed at least four mantle components DMM (depleted MORB mantle), HIMU (a mantle with high U/Pb ratio), EM-I and EM-II (enriched mantle; EM-I has lower $^{87}Sr/^{86}Sr$ values than EM-II). In addition to these four components, Hart et al. (1992) proposed another mantle component named FOZO for "focal zone" basalts. This component has been interpreted using two different models, but in both FOZO mixes in plumes containing enriched mantle (EM) and HIMU components one from the core-mantle boundary and the other from the lower mantle. The major difference between these two models is that in first model all components are derived from below 670 km, and in the other model it is derived from near the 670 km discontinuity itself. From the available isotopic data for the Jasra samples it is difficult to distinguish between these two models without some more isotopic data, particularly $^{206}Pb/^{204}Pb$, $^{207}Pb/^{204}Pb$, $^{208}Pb/^{204}Pb$, $^{3}He/^{4}He$ and noble gas data (Hart et al., 1992; Bell, 2002). The enriched mantle component may have been derived either from subducted crustal material in the mantle or from mantle metasomatism. But, as mentioned earlier, subduction-derived rocks should have negative Nb, Ta, and Ti anomalies; which is not observed in these rocks (Fig. 4). Thus, we prefer the mantle metasomatism model. Bell et al. (1998) pointed out that metasomatism is restricted mainly to the lithosphere, which can trap melt inclusions generated from the convecting asthenosphere. Bell (2001, 2002) suggested plume involvement in the genesis of carbonatitic, alkalic, and kimberlitic magmatism.

It is not easy to estimate the exact proportion of the different mantle components involved in generating the range of isotopic compositions preserved in the samples from the Jasra complex, but possibly mixing between the HIMU and enriched mantle components, similar to the FOZO model, could explain the range in Sr and Nd isotopic composition (Hart et al., 1992). The

isotope data are also consistent with mixing of other end members such as DMM or PREMA with EMI and EMII, or involvement of continental crust. Pb isotope data are probably required to distinguish between these possibilities. Mixing between HIMU and enriched mantle is noticed for many alkaline and carbonatite complexes (Tilton and Bell, 1994; Kramm and Kogarko, 1994; Bell and Simonetti, 1996; Kalt et al., 1997; Simonetti et al., 1995, 1998; Srivastava et al., 2005). Of course, to corroborate this observation, we require some more isotopic data particularly $^{206}Pb/^{204}Pb$, $^{207}Pb/^{204}Pb$, $^{208}Pb/^{204}Pb$, and $^{3}He/^{4}He$.

The Sung Valley alkaline carbonatite complex is thought to be contemporaneous with the Jasra and other alkaline-carbonatite complexes of Shillong plateau (Kumar et al., 1996; Ray et al., 1999; Heaman et al., 2002; Srivastava et al., 2005). $^{87}Sr/^{86}Sr_{initial}$ and $^{143}Nd/^{144}Nd_{initial}$ ratios obtained for Sung Valley complex are also plotted for comparison (Fig. 6a). Close isotopic similarities are observed between the silicate samples from both the complexes; the gabbro sample from Jasra shows exactly the same isotopic composition observed for an ijolitic sample from Sung Valley.

DISCUSSION

The main inferences from the field, petrological, geochemical, and radiogenic isotope data for samples from the Jasra complex, presented above, include (i) this early Cretaceous (U-Pb age is 105.2±0.5 Ma) alkaline-mafic-ultramafic complex consists of pyroxenite, gabbro, mafic dikes, and nepheline syenite, emplaced within the Proterozoic Shillong Group of the Shillong plateau, (ii) pyroxenites and gabbros do not show any direct field relationships while the mafic dikes, evidently contemporaneous with the gabbro, intrude granites as well as pyroxenites. These dikes do not cut the gabbro bodies. Nepheline syenite is the youngest unit of this complex and occurs as differentiates of gabbro or as small dike/dikelets, intruded into the pyroxenite with sharp edge contacts, (iii) primary calcite grains occur in the pyroxenite samples. Some thin

sections show ijolitic composition, (iv) the agpaitic indices of the nepheline syenites are < 1 indicating the miaskitic nature of these rocks and suggesting involvement CO_2 related activity in their genetic history, (v) the geochemical compositions of different rock units do not support any direct genetic relationship between the different rock types of complex, (vi) major element based discrimination function diagrams suggest ocean-island basalt (OIB) affinity, and (vii) Nd-Sr isotopic compositions suggest the involvement of an enriched mantle component in the genesis of the rocks studied.

From these observations, it appears that the different rock types of the Jasra complex do not have any co-genetic relationship. The overall alkaline nature of the different rock types and the miaskitic nature of the nepheline syenite samples of the Jasra complex indicate the involvement of CO_2 in their genesis. Harmer (1999) has presented a model for the genesis of such silicate rocks involving a primitive carbonate liquid, generated by low-degree melting of carbonated mantle peridotite. This model explains how such a melt contains appreciable alkalis and dissolves an adequate amount of olivine and pyroxene to provide the Al, Fe, and Si necessary for the crystallization of the silicate minerals. The other possibility may be through liquid immiscibility process but the relation of Mg# with Ba and La ratios precludes this possibility (Hamilton et al., 1989; Srivastava and Sinha, 2004; Srivastava et al., 2005). On the basis of experimental work on the immiscible carbonate liquid and associated silicate liquid under any temperature, pressure, and irrespective of whether the parental silicate melt was nephelinite or phonolite, Hamilton et al. (1989) shown that Ba/La ratio should be higher in immiscible carbonate melt than associated silicate melt.

As similar picture is observed in the present study, we favor Harmer's (1999) model for the genesis of the different rock types of the Jasra complex. Upton (1967) also pointed out that pyroxenite in alkalic environments may result from reaction between silicate rock and carbonatite magma. This model is also supported by the experimental work of Wallace and

Green (1988), Lee and Wyllie (1997), and Wyllie and Lee (1998). These workers showed that carbonate melts can be generated by direct melting of carbonated peridotite at depths equivalent to ~2-3.5 GPa, and are Mg-rich, and contain significant (up to 7%) amounts of alkalis and may, depending on the fertility of the peridotite and the Na/K balance, be in equilibrium with phlogophite ± paragasite-richterite amphibole (Wallace and Green, 1988; Sweeney, 1994). This deep-seated melt may consume orthopyroxene (lherzolite) and transform it into metasomatic clinopyroxene and olivine. During this process CO_2 is released and progressively metasomatizes the lherzolite to an alkaline wehrlite. With continued metasomatic enrichment, the alkali wehrlite melts to form an ultrabasic alkaline silicate magma that may crystallize to alkaline ultramafic-mafic rocks.

The isotopic data of the Jasra samples are plotted together with data for Kerguelen OIBs and Rajmahal tholeiites (Michard et al., 1986; Dosso et al., 1988; Storey et al., 1992; Mahoney et al., 1995) in Figure 6b. The data from the Jasra samples are similar to the isotopic compositions of the Kerguelen OIBs and Rajmahal Group II tholeiites. This observation is well supported by geochemical composition of these rocks (Fig. 5). A Kerguelen plume origin has been proposed for these basalts (Kent et al., 2002; Mahoney et al., 1992; Coffin et al., 2002; Duncan, 2002). On the basis of the temporal and spatial relationships of alkaline and carbonatite complexes of the Shillong plateau and radiogenic isotope compositions, it is suggested that a plume currently beneath Kerguelen was also responsible for these complexes (Ray et al., 1999; Heaman et al., 2002; Srivastava et al., 2005). The spatial and temporal relationship is clearly evident from Table 1 and Figure 1, which implies a genetic link between the ca. 107-115 Ma alkaline-carbonatite complexes in NE India with the Kerguelen OIBs.

Alkaline magma can also be generated in continental rift-like extensional tectonic environments (Wilson, 1989; Sheth et al., 2000; Winter, 2001; Verma, 2006). Although many features, such as OIB-like magma generated from an enriched mantle source, are similar in both

plume and extensional tectonics but none of the geological or geophysical feature noticed from the Shillong plateau suggest any possibility of extensional rift tectonics in the region. Thus, plume model for the genesis of Jasra samples seems more practical.

CONCLUSIONS

Field-relationships, geochemistry and the radiogenic compositions of the early Cretaceous Jasra alkaline-mafic-ultramafic complex suggest that different rock units (pyroxenite, gabbro and nepheline syenite) do not have any direct genetic relationship with one another and probably have different genetic histories. Discrimination function diagrams based on the major element data and radiogenic isotope data clearly suggest ocean-island basalt (OIB)-like origin for Jasra samples. Radiogenic isotopic compositions suggest that these rocks are derived from mixing of mantle components like HIMU and enriched mantle. Low-degree melting of a metasomatized mantle peridotite produces carbonatite melts that might dissolve an adequate amount of olivine and pyroxene to provide the Al, Fe, and Si necessary for crystallization of silicate minerals. CO_2 released by this process progressively metasomatizes the lherzolite to an alkaline wehrlite and melts derived from alkaline wehrlite (ultrabasic alkaline silicate magma) may be responsible for crystallisation of different rocks of the Jasra complex. This genetic history suggests that the Jasra alkaline-mafic-ultramafic complex is an integrated part of alkaline-carbonatite magmatism of the Shillong plateau and closely associated with Kerguelen plume activity.

References

Acharya, S.K., Mitra, N.D. and Nandy, D.R., 1986, Regional geology and tectonic setting of northeast India and adjoining region: Geological Survey of India Memoir, v. 119, p. 6-12.

Agrawal, S., Guevara, M. and Verma, S.P., 2004, Discriminant analysis applied to establish major-element field boundaries for tectonic varieties of basic rocks: International Geology Review, v. 46, p. 575-594.

Baksi, A.K., 1995, Petrogenesis and timing of volcanism in the Rajmahal flood basalt province, Northeastern India: Chemical Geology, v. 121, p. 73-90.

Bates, R.L. and Jackson, J.A., 1980, Glossary of Geology: Americal Geological Institute, Falls Church, Virginia, 2nd Ed, 751p.

Bell, K., 2001, Carbonatites: relationships to mantle-plume activity, *in* Ernst, R.E. and Buchan, K.L., eds., Mantle Plumes: Their Identification Through Time: Geological Society of America Special Paper 353, p. 267-290.

Bell, K., 2002, Probing the mantle: the story from carbonatites: EOS, v. 83, p. 273-277.

Bell, K. and Simonetti, A., 1996, Carbonatite magmatism and plume activity: implications from the Nd, Pb, and Sr isotope systematics of Oldoinyo Lengai: Journal of Petrology, v. 37, p. 1321-1339.

Bell, K., Kjarsgaard, B.A. and Simonetti, A., 1998, Carbonatites – Into the twenty-first Century: Journal of Petrology, v. 39, p. 1839-1845.

Carlson, R.W., 1991, Physical and chemical evidence on the cause of source characteristics of flood basalt volcanism: Australian Journal of Earth Sciences, v. 38, p. 525-544.

Coffin, M.F., Pringle, M.S., Duncan, R.A., Gladezenko, T.P., Storey, M., Müller, R.D. and Gahagan, L.A., 2002, Kerguelen hotspot magma output since 130 Ma: Journal of Petrology, v. 43, p. 1121-1139.

Cullers, R.L. and Graf, J.L., 1984, Rare-earth elements in igneous rocks of the continental crust: predominantly basic and ultrabasic rocks, *in* Henderson, P., ed., Rare Earth Element Geochemistry: Amsterdam, Elsevier, p. 237-274.

Das Gupta, A.B. and Biswas, A.K., 2000, Geology of Assam: Geological Society of India, Bangalore, 169p

DePaulo, D.J., 1988, Neodymium isotope geochemistry: an introduction: Springer Verlag, New York.

Desikachar, S.V., 1974, A review of the tectonic and geological history of eastern India in terms of plate tectonic theory: Journal of Geological Society of India, v. 15, p. 137-149.

Dickin, A.P., 1995, Radiogenic Isotope Geology: Cambridge, Cambridge University Press, 490 p.

Dosso, L., Bougault, H., Beuzart, P., Calvez, J.–Y. and Joron, J.–L., 1988, The geochemical structure of the South East Indian Ridge: Earth and Planetary Science Letters, v. 88, p. 47-59.

Duncan, R.A., 2002, A time frame for construction of the Kerguelen Plateau and Broken Ridge: Journal of Petrology, v. 43, p. 1109-1119.

Evans, P., 1964, The tectonic framework of Assam. Journal of Geological Society of India, v. 5, p. 80-96.

Evensen, N.M., Hamilton, P.J. and O'Nion, R.K., 1978, Rare earth abundances in chondritic meteorites: Geochimica et Cosmochimica Acta, v. 42, p. 1199-1212.

Faure, G., 1986, Principles of Isotope Geology: New York, Wiley, 653 p.

Faure, G., 2001, Origin of Igneous Rocks – The isotopic Evidence: Berlin, Springer, 496 p.

Franz, G., Steiner, G., Volker, F., Pudlo, D. and Hammerschmidt, K., 1999, Plume related alkaline magmatisn in central Africa – the Meidob Hills (W Sudan): Chemical Geology, v. 157, p. 27-47.

Frey, F.A., McNaughton, N.J., Nelson, D.R., de Laeter, J.R. and Duncan, R.A., 1996, Petrogenesis of the Bunbury basalt, Western Australia: interaction between the Kerguelen plume and Gondwana lithosphere?: Earth and Planetary Science Letters, v. 141, p. 163-183.

Frey, F.A., Coffin, M.F., Wallace, P.J., Weis, D. and ODP Leg 183 Shipboard Scientific Party, 2000, Origin and evolution of a submarine large igneous province: the Kerguelen plateau and Broken Ridge, southern Indian Ocean: Earth and Planetary Science Letters, v. 176, p. 73-89.

Ghosh, S., Chakrabarty, S., Paul, D.K., Bhalla, J.K., Bishui, P.K. and Gupta, S.N., 1994, New Rb-Sr isotopic ages and geochemistry of granitoids from Meghalaya and their significance in middle to late Proterozoic crustal evolution: Indian Minerals, v. 48, p. 33-44.

Golani, P.R., 1991, Nangcharam fault: a major dislocation zone from western Meghalaya: Journal of Geological Society of India, v. 37, p. 31-38.

Goldstein, S.L., O'Nions, R.K. and Hamilton, P.J., 1984, A Sm-Nd study of atmospheric dusts and particles from major river systems: Earth and Planetary Science Letters, v. 70, p. 221-236.

Green, D.H., 1971, Composition of basaltic magmas as indicators of conditions of origin: application to oceanic volcanism: Philosophical Transaction of Royal Society of London, v. 268A, p. 707-725.

Gupta, R.P. and Sen, A.K., 1988, Imprints of Ninety-East Ridge in the Shillong Plateau, Indian Shield: Tectonophysics, v. 154, p. 335-341.

Hamilton, D.L., Bedson, P. and Esson, J., 1989, The behavior of trace elements in the evolution of carbonatites, *in* Bell, K., ed., Carbonatites – Genesis and Evolution: London, Unwin Hyman, p. 405-427.

Harmer, R.E., 1999, The petrogenetic association of carbonatite and alkaline magamatism: constraints from the Spitskop Complex, South Africa: Journal of Petrology, v. 40, p. 525-548.

Hart, S.R., 1988, Heterogeneous mantle domains: signatures, genesis and mixing chronologies: Earth and Planetary Science Letters, v. 90, p. 273-296

Hart, S.R., Hauri, E.H., Oschmann, L.A. and Whitehead, J.A., 1992, Mantle plumes and entrainment: isotopic evidence: Science, v. 256, p. 517-520.

Heaman, L.M., Srivastava, R.K. and Sinha, A.K., 2002, A precise U-Pb zircon/baddeleyite age for the Jasra igneous complex, Karb-Analong district, Assam, NE India: Current Science, v. 82, p. 744-748.

Heinrich, E. Wm., 1966, The Geology of Carbonatites: Rand Mcnally and Company, Chicago, 555 p.

Jacobsen, S.B. and Wasserburg, G.J., 1980, Sm-Nd isotopic evolution of chondrites. Earth and Planetary Science Letters, v. 50, p. 139-155.

Kalt, A., Hegner, E. and Satir, M., 1997, Nd, Sr and Pb isotopic evidence for diverse mantle sources of East Africa Rift carbonatites: Tectonophysics, v. 278, p. 31-45.

Kayal, J.R., Arefiev, S.S., Barua, S., Hazarika, D., Gogoi, N., Kumar, A., Chowdhury, S.N. and Kalita, S., 2006, Shillong plateau earthquakes in northeast India region: complex tectonic model: Current Science, v. 91, p. 109-114.

Kent, R.W., 1995, Continental and oceanic flood basalt provinces: current and future perspectives, *in* Srivastava, R.K. and Chandra, R., eds., Magmatism in Relation to Diverse Tectonic Settings: Rotterdam, A.A.Balkema, p. 17-42.

Kent, R.W., Saunders, A.D., Kempton, P.D. and Ghose, N.C., 1997, Rajmahal basalts, eastern India: mantle sources and melt distribution at a volcanic rifted margin. *In* Mahoney, J.J. and Coffin, M.F., eds., Large Igneous Provinces: Continental, Oceanic and Planetary Flood Volcanism: Geophysical Monograph, American Geophysical Union, v. 100, p. 145-182.

Kent, R.W., Pringle, M.S., Müller, R.D., Saunders, A.D. and Ghose, N.C., 2002, 40Ar/39Ar geochronology of the Rajmahal basalts, India, and their relationship to the Kerguelen Plateau: Journal of Petrology, v. 43, p. 1141-1153.

Kramm, U. and Kogarko, L.N., 1994, Nd and Sr isotope signatures of the Khibina and Lovozero agpaitic centers, Kola alkaline province, Russia: Lithos, v. 32, p. 225-242.

Kumar, D., Mamallan, R. and Diwedy, K.K., 1996, Carbonatite magmatism in northeast India: Journal of Southeast Asian Earth Sciences, v. 13, p. 145-158.

Lee, W.J. and Wyllie, P.J., 1997, Liquid immiscibility in the join $NaAlSiO_4$-$NaAlSiO_8$-$CaCO_3$ at 1 Gpa: Implications for crustal carbonatites: Journal of Petrology, v. 98, p. 1113-1135.

Le Bas, M.J., 1987, Nephilinites and carbonatites, *in* Fitton, J.G. and Upton, B.G.J., eds., Alkaline Igneous Rocks: Geological Society of London Special Publication 30, p.53-83.

Le Bas, M.J., 1989, Diversification of carbonatite, *in* Bell, K., ed., Carbonatites – Genesis and Evolution: London, Unwin Hyman, p. 428-447.

Le Maitre, R.W., 2002, Igneous Rocks: A classification and glossary of terms: 2nd Ed., Cambridge University Press, Cambridge, 236 p.

Luhr, J.F., 1997, Extensional tectonics and the diverse primitive volcanic rocks in the western Mexican volcanic belt: Canadian Mineralogist, v. 35, p. 473-500.

Mahoney, J.J., Macdougall, J.D., Lugmair, G.W., Gopalan, K. and Krishnamurthy, P., 1985, Origin of contemporaneous theleiitic and K-rich alkalic lavas: a case study from the northern Deccan plateau, India: earth and Planetary Letters, v. 72, p. 39-53.

Mahoney, J.J., le Roex, A.P., Peng, Z., Fisher, R.L. and Natland, J.H., 1992, Southwestern limits of Indian Ocean Ridge mantle and the origin of low $^{206}Pb/^{204}Pb$ mid-ocean ridge basalt: Isotope systematics of the Central Southwest Indian Ridge (17º-50ºE): Journal of Geophysical Research, v. 97, p. 19771-19790.

Mahoney, J.J., Jones, W.B., Frey, F.A., Salters, V.J. M., Pyle, D.G. and Davies, H.L., 1995, Geochemical characteristics of lavas from Broken Ridge, the Naturaliste Plateau and southernmost Kerguelen Plateau: Cretaceous plateau volcanism in the southeast Indian Ocean: Chemical Geology, v. 120, p. 315-345.

Mamallan, R., Kumar, D. and Bajpai, R.K., 1994, Jasra ultramafic-mafic-alkaline complex: a new find in the Shillong plateau, northeastern India: Current Science, v. 66, p. 64-65.

Mazumdar, S.K., 1976, A summary of the Precambrian geology of the Khasi Hills, Meghalaya: Geological Survey of India Miscellaneous Publication, v. 23 (2), p. 311-334.

McDonough, W.F., Sun, S.–S., Ringwood, A.E., Jagoutz, E. and Hofmann, A.W., 1992, K, Rb and Cs in the earth and moon and the evolution of the earth's mantle: Geochimica et Cosmochimica Acta, v. 56, p. 1001-1012.

Michard, A., Montigny, R. and Schlich, R., 1986, Geochemistry of the mantle beneath the Rodriguez triple junction and the South-East Indian Ridge: Earth and Planetary Science Letters, v. 78, p. 104-114.

Middlemost, E.A.K., 1989, Iron oxidation ratios, norms and the classification of volcanic rocks: Chemical Geology, v. 77, p. 19-26.

Nandy, D.R., 1980, Tectonic patterns in northeastern India: Indian Journal of Earth Sciences, v. 7, p. 103-107.

Pyle, D.G., Christie, D.M., Mahoney, J.J. and Duncan, R.A., 1995, Geochemistry and geochronology of ancient southeast Indian Ocean and southwest Pacific Ocean seafloor: Journal of Geophysical Research, v. B100, p. 22261-22282.

Ray, J.S., Ramesh, R. and Pande, K., 1999, Carbon isotopes in Kerguelen plume-derived carbonatites: evidence for recycled inorganic carbon: Earth and Planetary Science Letters, v. 170, p. 205-214.

Ray, J.S., Trivedi, J.R. and Dayal, A.M., 2000, Strontium isotope systematics of Amba Dongar and Sung Valley carbonatite-alkaline complexes, India: evidence for liquid immiscibility, crustal contamination and long-lived Rb/Sr enriched mantle source: Journal of Asian Earth Sciences, v. 18, p. 585-594.

Sarkar, A., Datta, A.K., Poddar, B.K., Bhattacharyya, B.K., Kollapuri, V.K. and Sanwal, R., 1996, Geochronological studies of Mesozoic igneous rocks from eastern India: Journal of Southeast Asian Earth Sciences, v. 13, p. 77-81.

Saunders, A.D., Storey, M., Kent, R.W. and Norry, M.J., 1992, Consequences of plume-lithosphere interactions, *in* Storey, B.C., Alabaster, T. and Pankhurst, R.T., eds., Magmatism and the Causes of Continental Break-up: London, Geological Society of London Special Publication 68, p. 41-60.

Sheth, H.C., Torres-Alvarado, I.S. and Verma, S.P., 2000, Beyond subduction and plumes: a unified tectono-petrogenetic model for the Mexican volcanic belt: International Geology Review, v. 42, p. 1116-1132.

Simonetti, A., Bell, K. and Viladkar, S.G., 1995, Isotopic data from the Amba Dongar Carbonatite Complex, west-central India: Evidence for an enriched mantle source: Chemical Geology, v. 122, p. 185-198.

Simonetti, A., Goldstein, S.L., Schmidberger, S.S. and Viladkar, S.G., 1998, Geochemical and Nd, Pb and Sr Isotope data from Deccan alkaline complexes- Inferences for mantle sources and plume-lithosphere interaction: Journal of Petrology, v. 39, p. 1847-1864.

Srivastava, R.K. and Sinha, A.K., 2004, Geochemistry of early Cretaceous alkaline ultramafic-mafic complex from Jasra, Karbi Anglong, Shillong plateau, Northeastern India: Gondwana Research, v. 7, p. 549-561.

Srivastava, R.K., Heaman, L.M., Sinha, A.K. and Shihua, S., 2005, Emplacement age and isotope geochemistry of Sung Valley Alkaline-Carbonatite complex, Shillong Plateau, Northeastern India: implications for primary carbonate melt and genesis of the associated silicate rocks: Lithos, v. 81, p. 33-54.

Storey, M., Kent, R.W., Saunders, A.D., Hergt, J., Salters, V.J.M., Whitechurch, H., Sevigny, J.H., Thirlwall, M.F., Leat, P., Ghose, N.C. and Gifford, M., 1992, Lower Cretaceous volcanic rocks on continental margins and their relationship to the Kerguelen Plateau: Proceedings Ocean Drilling Program Scientific Results, v. 120, p. 33-53.

Sweeney, R.J. (1994) Carbonatite melt compositions in the earth's mantle. Earth and Planetary Science Letters 128, 259-270.

Tilton, G. R. and Bell, K., 1994, Sr-Nd Pb isotope relationships in Late Archean carbonatites and alkaline complexes: applications to the geochemical evolution of the Archean mantle: Geochimica et Cosmochimica Acta, v. 58, p. 3145-3154.

Upton, B.G.J., 1967, Alkaline pyroxenites, *In* Wyllie, P.J., ed., Ultramafics and Related Rocks: New York, John Wiley & Sons, p. 281-288.

Velasco-Tapia, F. and Verma, S.P., 2001, First partial meeting inversion model for a rift-related origin of the Sierra de Chichinautzin volcanic field, central Mexican volcanic belt: International Geology Review, v. 43, p. 788-817.

Verma, S.P., 2006, Extensión-related origin of magmas from a garnet-bearing source in the Los Tuxtlas volcanic field, Mexico: International Journal of Earth Sciences, v. 95, p. 871-901.

Verma, S.P., Torres-Alvarado, I.S. and Sotelo-Rodríguez, Z.T., 2002, SINCLAS: standard igneous norm and volcanic rock classification system: Computer Geoscience, v. 28, p. 711-715.

Verma, S.P., Guevara, M. and Agrawal, S., 2006, Discriminating four tectonic settings: Five new geochemical diagrams for basic and ultrabasic volcanic rocks based on log-ratio transformation of major-element data. Journal of Earth System Science, v. 115, p. 485-528.

Wallace, M.E. and Green, D.H., 1988, An experimental determination of primary carbonatite magma composition: Nature, v. 335, p. 343-346.

Wilson, M., 1989, Igneous Petrogenesis: London, Chapman & Hall, 466 p.

Winter, J.D., 2001, An Introductioin to Igneous and Metamorphic Petrology: New Jersey, Prentice Hall, 697 p.

Wyllie, P.J. and Lee, W.-J., 1998, Model system controls on conditions for formation of magnesiocarbonatite and calciocarbonatite magmas from the mantle: Journal of Petrology, v. 39, p. 1885-1893.

Zindler, A. and Hart, S.R., 1986, Chemical geodynamics. Annals Review Earth and Planetary Sciences, v. 14, p. 493-571.

Explanation of the figures

Figure 1: Map showing location of magmatic activity of the Kerguelen Plateau, Broken Ridge, Naturaliste Plateau, Bunbury, Rajmahal-Sylhet, and associated ultramafic-alkaline-carbonatite complexes of Shillong Plateau (modified after Kent et al., 2002). Age data for these magmatic rocks are presented in Table 1.

Figure 2: (a) Regional geological and tectonic set-up of the Shillong Plateau (modified after Srivastava and Sinha, 2004). 1. Cretaceous-Tertiary sediments, 2. Ultramafic-alkaline-carbonatite complexes, 3. Sylhet basalts, 4. Archaean gneissic complex, Shillong Group rocks, mafic igneous rocks, and Proterozoic granites, 5. Major fault-systems, and 6. Alluvium and recent sediments. **(b)** Geological map of the Jasra alkaline ultramafic-mafic complex (after Srivastava and Sinha, 2004). 1. Shillong Group rocks, 2. Neoproterozoic granite, 3. Pyroxenite, 4. Gabbro, 5. mafic dike exposures, 6. Nepheline syenite exposures. Locations of geochemically analysed samples are marked on the map.

Figure 3: Variation diagram plotted between Mg number and SiO_2, Nb, and Zr and SiO_2 and Zr.

Figure 4: Primordial-mantle-normalized multi-element and chondrite-normalized rare-earth element patterns for different samples from the Jasra complex. Primordial mantle and chondrite values are taken from McDonough et al. (1992) and Evenson et al. (1978) respectively.

Figure 5: Discrimination function diagrams for the Jasra samples (After Verma et al., 2006). The per cent given next to the tectonic setting name represents the percent success obtained for the Jasra samples.

Figure 6: (a) $^{143}Nd/^{144}Nd$ and $^{87}Sr/^{86}Sr$ isotope correlation plot, showing the main oceanic mantle components of Zindler and Hart (1986). The mantle array is defined by many MORB and ocean island basalts, and bulk Earth values of $^{143}Nd/^{144}Nd$ and $^{87}Sr/^{86}Sr$ can be observed from this trend (Faure, 1986, 2001; Dickin, 1995). Isotopic data of Sung Valley samples are taken from Srivastava et al. (2005). Kerguelen plateau basalt field is based on data from Michard et al. (1986), Dosso et al. (1988), Storey et al. (1992) and Mahoney et al. (1995). **(b)** $^{87}Sr/^{86}Sr_{initial}$ and εNd plot for the studied samples and the Kerguelen Plateau basalts. Source for Kerguelen data is same as mentioned above.
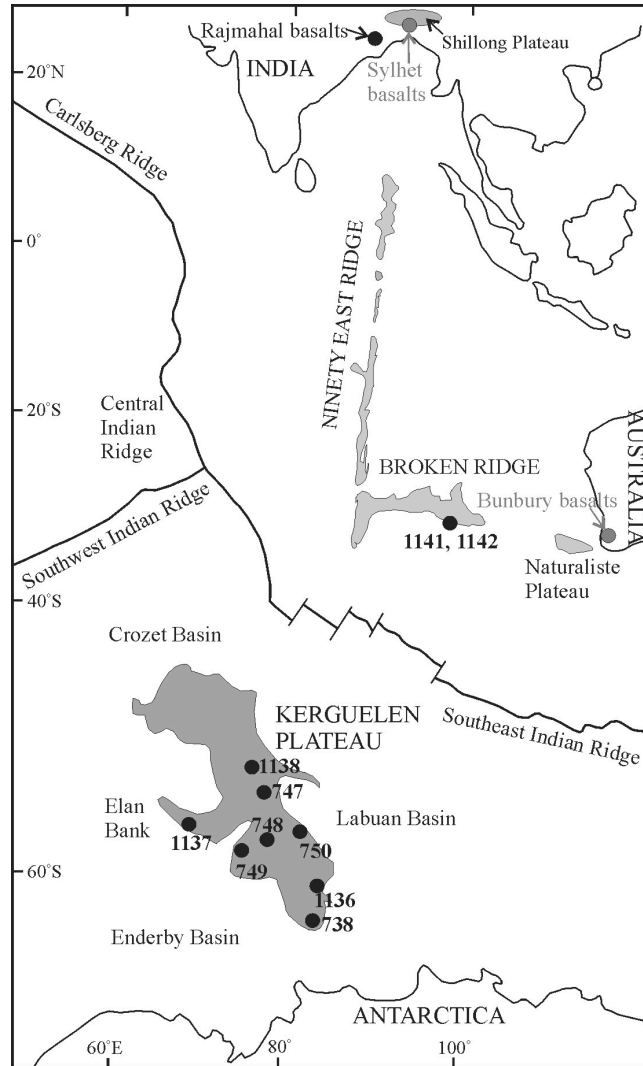
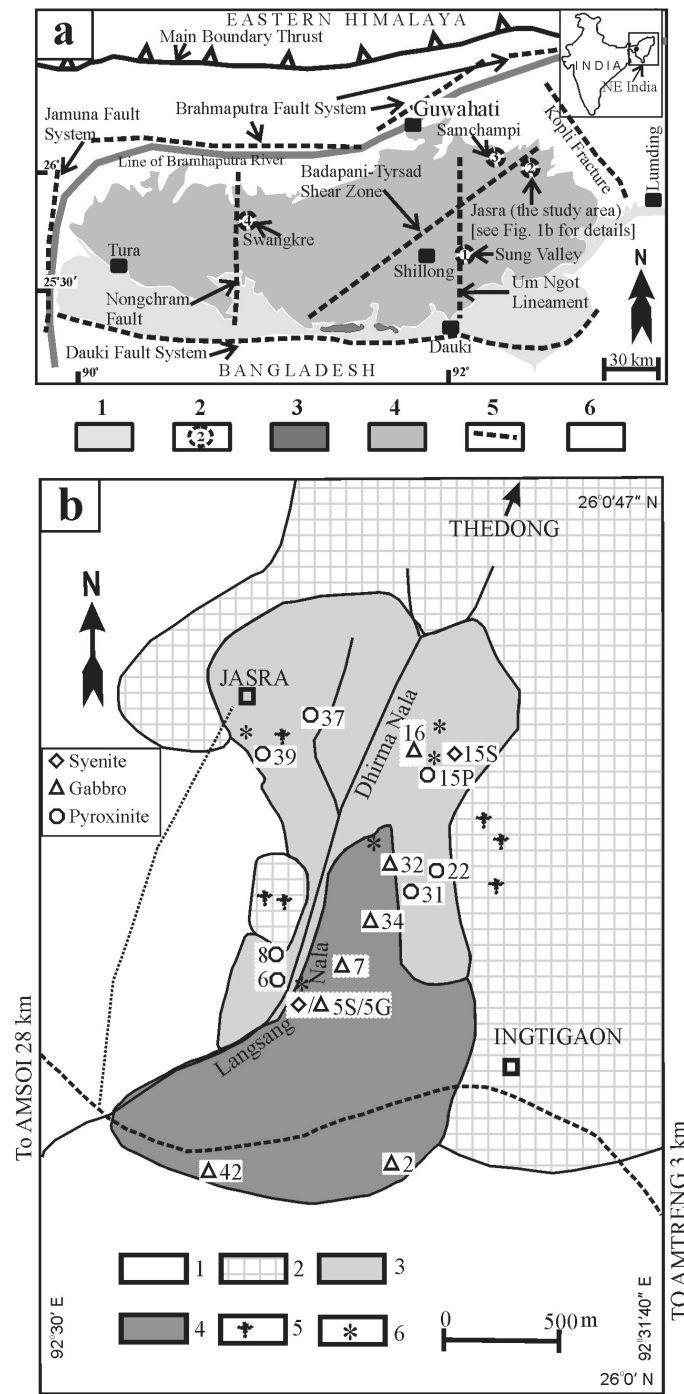Figure 1: Srivastava and Sinha

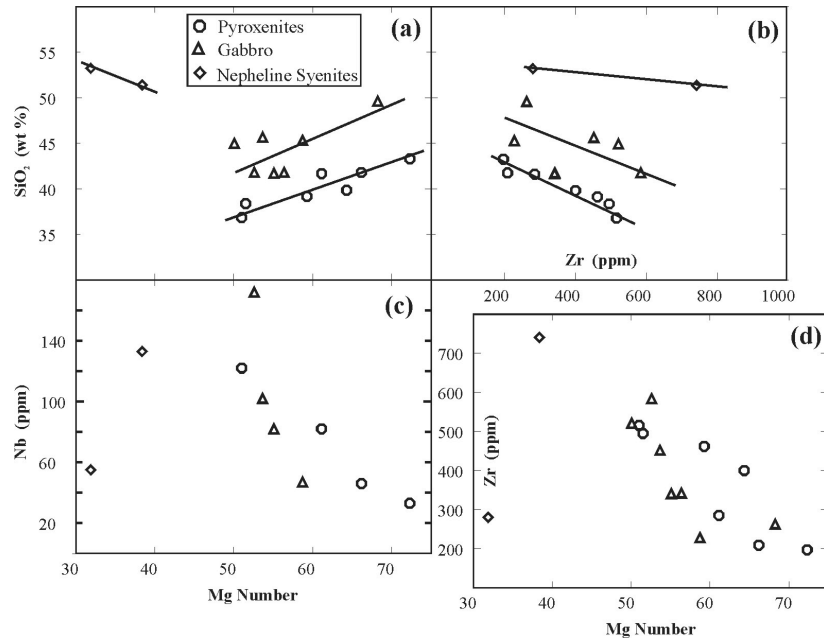Figure 2: Srivastava and Sinha

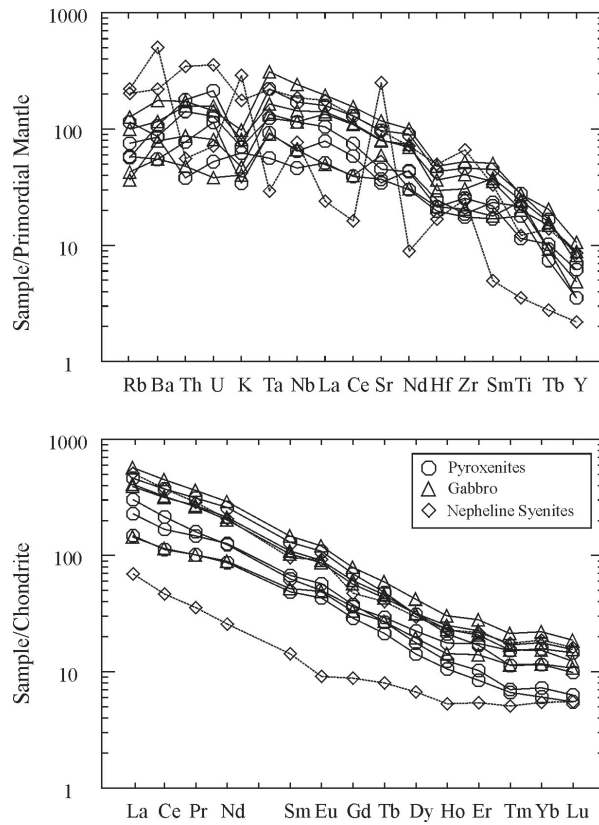Figure 3: Srivastava and Sinha
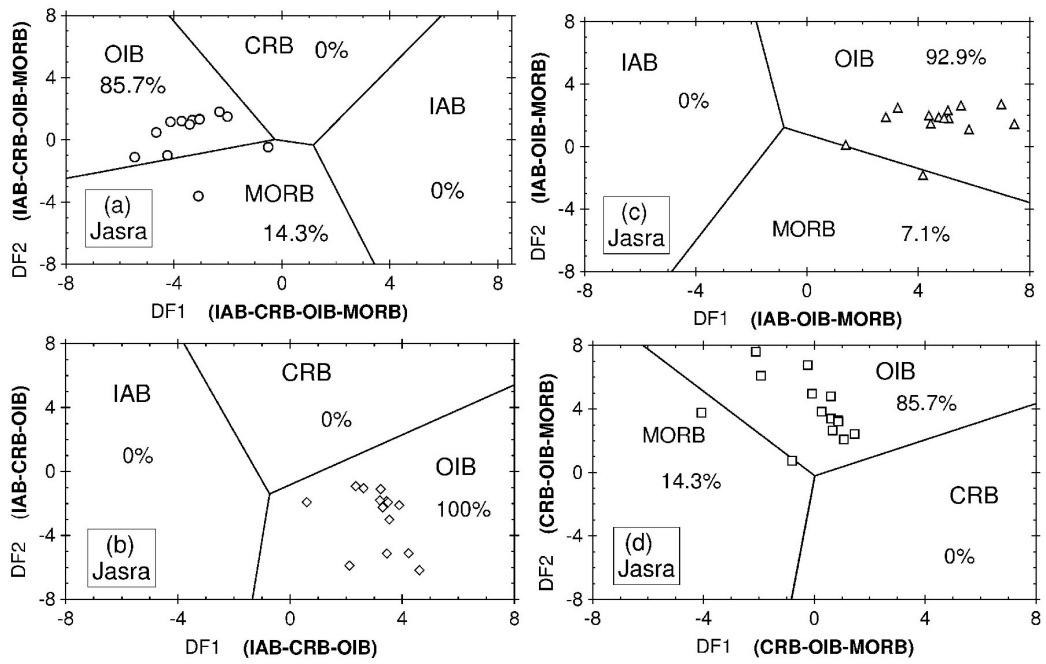

Figure 4: Srivastava and Sinha

Figure 5: Srivastava and Sinha
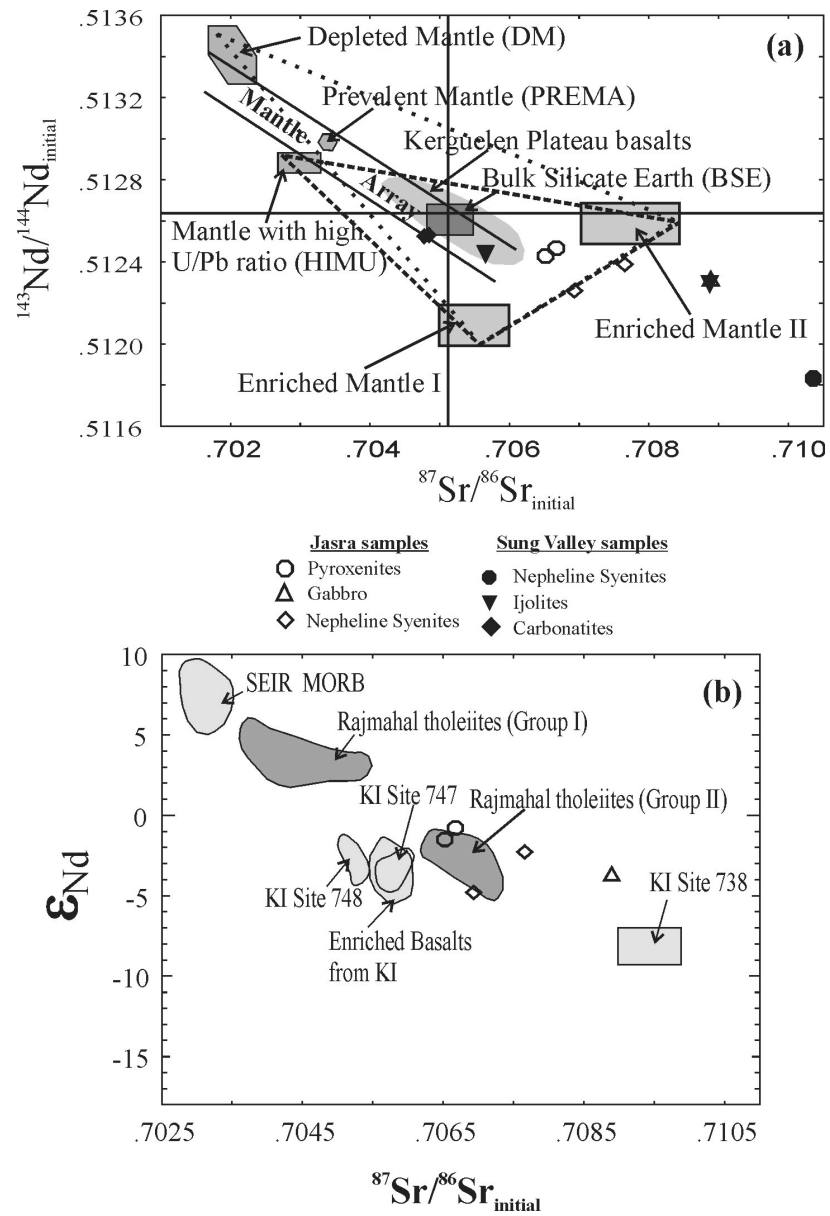
Figure 6: Srivastava and Sinha

Table 1: Age data on basalts from the Kerguelen Plateau, Broken Ridge, Naturaliste Plateau, Bunbury, and Rajmahal-Sylhet Igneous Province and associated ultramafic-alkaline-carbonatite complexes of Shillong Plateau. See Figure 6 for their locations.

Method	Material	Age (in Ma)	References
Kerguelen Plateau			
	Basalt from ODP site 1136	118-119	
Ar-Ar	Basalt from ODP site 1137	107-108	Coffin *et al.* (2002); Duncan
	Basalt from ODP sites 749 and 750	110-112	(2002)
	Basalt from ODP site 1138	~100	
Broken Ridge			
Ar-Ar	Basalt from ODP sites 1141 and 1142	~100	Coffin *et al.* (2002); Duncan (2002)
Naturaliste Plateau			
Ar-Ar	Basalt	100.6±1.2	Pyle *et al.* (1995)
Bunbury, Western Australia			
Ar-Ar	Basalt lava	123-130	Frey *et al.* (1996); Coffin *et al.* (2002)
Rajmahal-Sylhet Flood Basalts Province			
Ar-Ar	Basalts	105-118	Baksi (1995); Kent *et al.* (2002); Coffin *et al.* (2002)
Ultramafic-alkaline-carbonatite complexes (Shillong Plateau)			
1. Sung Valley			
Ar-Ar	Pyroxenite (WR) and phlogopite from carbonatite	107.2±0.8	Ray *et al.* (1999)
Rb-Sr	Carbonatite (WR), pyroxenite (WR), and phlogopite from carbonatite	106±11	Ray *et al.* (2000)
U-Pb	Perovskite from ijolite	115.1±5.1	Srivastava *et al.* (2005)
2. Jasra			
U-Pb	Zircon and baddeleyite from differentiated gabbro	105.2±0.5	Heaman *et al.* (2002)
3. Samchampi			
Fission track	Apatite	~ 105	Acharya *et al.* (1986)
4. Swangkre			
K-Ar	Lamprophyre	107±3	Sarkar *et al.* (1996)

Table 2: Petrographic characters of different igneous rock units associated to the Jasra alkaline-mafic-ultramafic complex.

Rock Type (oldest to youngest)	Mineral compositions (in the order of abundance)	Texture	Colour Index
Pyroxenite (oldest unit)	Clinopyroxenes (68-74%; diopside, aegirine-augite, aegirine, augite, and titan-augite), opaques (~12%; magnetite and ilmanite), olivine, biotite, orthoclase, plagioclase, apatite, sphene, and calcite	Hypidiomorphic and porphyritic	~94
Alkaline pyroxenite	Clinopyroxenes (54-57%; diopside, aegirine-augite, aegirine, augite, and titan-augite), olivine (10-14%), nepheline (5-10%), opaques (magnetite and ilmanite), biotite, orthoclase, plagioclase, apatite, sphene, and calcite	Hypidiomorphic and porphyritic	80-85
Essexite	Clinopyroxenes (44-60%; augite, titan-augite, aegirine-augite, aegirine, and diopside), feldspars (24-35%; plagioclase, orthoclase), olivine, nepheline (5-9%), opaques (magnetite and ilmanite), apatite, sphene, biotite, zircon, and rutile.	Hypidiomorphic and panidiomorphic	57-66
Olivine Gabbro & mafic dikes	Clinopyroxenes (~36%; augite, titan-augite, aegirine-augite, aegirine, and diopside), plagioclase (~38%), olivine (~7%), opaques (magnetite and ilmanite), orthoclase (4%), nepheline (4%), apatite, sphene, biotite, zircon, and rutile.	Hypidiomorphic and panidiomorphic textures in Gabbro samples and intergranular or ophitic textures in dike samples	~50
Nepheline syenite (differentiated gabbro)	Orthoclase (~46%), plagioclase (~15%), clinopyroxenes (~13%; aegirine, aegirinie-augite, and augite), nepheline (~8%), biotite, opaques (magnetite and ilmanite), calcite, zircon, sphene, apatite, and olivine.	Hypidiomorphic, porphyritic, and poikilitic	~25
Nepheline syenite dikes (youngest unit)	Orthoclase (~60%), plagioclase (~10%), clinopyroxenes (~9%; aegirine, aegirinie-augite, and augite), nepheline (~6%), biotite, opaques (magnetite and ilmanite), calcite, zircon, sphene, apatite, and olivine.	Hypidiomorphic, porphyritic, and poikilitic	~19

Table 3: Whole rock major (wt% oxides) and CIPW Norm compositions of different rock units of the Jasra alkaline-mafic-ultramafic complex.

S.No.→	Pyroxenites							Gabbros							Ne Syenites	
	JS/6	JS/8	JS/15P	JS/22	JS/31	JS/37	JS/39	JS/2	JS/5G	JS/7	JS/16	JS/32	JS/34	JS/42	JS/5S	JS/15S
SiO$_2$	43.29	39.85	41.79	41.67	39.18	36.84	38.40	41.71	45.68	44.98	49.62	41.48	45.32	41.79	51.40	53.24
TiO$_2$	3.81	4.76	4.62	2.54	6.14	5.94	5.67	5.19	4.24	4.65	2.52	5.84	5.05	4.87	2.60	0.76
Al$_2$O$_3$	5.72	7.72	5.55	8.64	5.99	8.87	9.82	9.10	11.08	11.01	5.94	9.58	11.34	9.18	16.29	19.18
Fe$_2$O$_3$	12.37	14.60	13.35	13.98	15.86	16.08	15.36	16.00	14.21	14.93	9.50	13.80	13.68	15.51	10.07	4.78
MnO	0.16	0.21	0.14	0.24	0.23	0.23	0.22	0.23	0.22	0.22	0.19	0.23	0.16	0.22	0.15	0.07
MgO	14.36	11.26	11.62	9.41	10.26	7.16	6.98	8.40	6.54	6.41	8.74	6.55	8.33	8.58	2.33	0.83
CaO	16.44	15.31	19.31	14.70	17.23	16.34	14.56	14.21	10.88	10.82	17.69	13.65	11.39	13.58	4.81	4.39
Na$_2$O	1.02	1.62	0.78	2.97	1.03	2.92	3.49	2.33	3.01	3.03	1.49	2.75	2.32	2.33	4.61	3.22
K$_2$O	1.80	1.51	0.99	2.04	1.57	2.02	2.21	1.36	2.34	2.52	2.36	2.82	1.16	1.55	5.12	8.40
P$_2$O$_5$	0.31	0.76	0.34	0.35	0.94	1.08	1.07	1.33	0.94	1.00	0.36	0.98	0.26	1.08	0.78	0.06
LOI	1.08	1.33	1.22	2.14	0.59	1.27	1.22	--	--	--	0.99	1.08	--	--	0.70	3.90
Total	100.36	98.93	99.71	98.68	99.02	98.75	99.00	99.86	99.14	99.57	99.40	98.76	99.01	98.69	98.86	98.83
Mg#	72.30	64.32	66.18	61.14	59.26	51.00	51.51	55.10	53.66	50.09	68.26	52.60	58.74	56.39	38.40	31.88
Al															8.62	10.15
Na															3.42	2.39
K															4.25	6.97
A.I.*															0.60	0.40
A.I.**															0.89	0.92
CIPW Norm																
Or								8.16	14.11	15.15	14.29	8.21	7.01	9.41	31.06	52.49
Ab								3.98	16.29	12.78	4.23		18.81	3.50	28.55	11.67
An	5.82	9.69	8.96	4.42	7.30	5.33	4.77	10.51	10.01	9.15	2.62	5.67	17.48	10.28	8.86	13.81
Lc	8.49	7.26	4.71	9.91	7.50	9.74	10.62									
Ne	4.76	7.71	3.68	14.28	4.87	13.93	16.58	8.69	5.25	9.20	4.70	13.06	0.68	9.07	6.22	9.29
Di	49.46	43.46	52.42	45.44	46.17	33.39	38.45	42.49	31.54	31.79	66.25	46.89	31.11	41.98	8.61	9.42
Ol	17.07	14.24	11.25	12.51	11.72	10.07	7.49	9.45	7.90	9.22		2.07	11.41	10.17	5.79	1.71
Mt	2.17	3.35	2.37	3.24	2.82	3.70	3.52	3.59	4.47	3.36	2.15	3.16	3.09	3.52	3.97	1.94
Il	7.37	9.38	9.02	5.06	12.02	11.74	11.16	10.01	8.22	8.98	4.90	11.49	9.80	9.50	5.07	1.53
Ap	0.73	1.83	0.81	0.85	2.25	2.60	2.57	3.13	2.22	2.36	0.86	2.35	0.62	2.57	1.86	0.15
Cs	4.12	3.09	6.80	4.28	5.36	9.50	4.84									
Rock type	PIC	BSN (mnp)	PB	BSN (mnp)	FOI (mnp)	FOI (mnp)	FOI (mnp)	TEP (mnp)	TB (pot)	TEP (bsn)	B (alk)	TEP (mnp)	B (alk)	BSN (mnp)	TPH	TPH

(--) either zero or below zero; A.I. (Agpaitic Index); *[(Na$_2$O+K$_2$O)/Al$_2$O$_3$]; ** [(Na+K)/Al]; PIC: Picrite; BSN (mnp): Basanite (melanephelinite); PB: Picrobasalt; FOI (mnp): Foidite (melanephelinite); TEP (mnp): Tephrite (melanephelinite); TB (pot): Potassic trachybasalt; TEP (bsn): Tephrite (basanite); B (alk): Alkali basalt; TPH: Tephriphonolite.

Table 4: Trace and rare-earth (ppm) elements analyses of different rock units of the Jasra alkaline-mafic-ultramafic complex.

S.No.→	Pyroxenites				Gabbros				Ne Syenites	
	JS/6	JS/15P	JS/22	JS/37	JS/2	JS/5G	JS/32	JS/34	JS/5S	JS/15S
Cr	1080	104	504	21	178	-	126	91	-	-
Ni	194	179	166	147	106	-	151	158	-	-
Sc	37	42	21	23	25	20	20	28	6	2
V	286	308	414	465	409	337	439	583	98	181
Rb	48	37	73	36	23	129	80	27	129	141
Ba	595	384	605	746	549	809	1225	385	1540	3542
Sr	781	727	954	2052	1666	1690	2473	1252	2021	5312
Ga	14	15	16	23	20	25	20	18	25	24
Ta	2.3	3.8	5.1	9.1	5.5	6.7	12.7	3.7	9.0	1.2
Nb	33	46	82	122	82	133	172	47	133	55
Hf	6.1	7.6	6.6	13.3	9.1	11.2	14.7	6.6	15.4	5.2
Zr	197	209	285	516	341	452	584	228	741	280
Y	16	16	28	32	37	40	48	22	39	10
Th	3.2	6.5	11.9	15.0	7.3	13.2	14.5	4.0	29.1	4.7
U	1.1	2.4	2.7	4.5	1.7	3.3	3.0	0.8	7.5	1.5
La	36.2	55.8	74.1	113.0	94.8	99.0	138.0	35.0	125.0	17.0
Ce	71.9	107.0	137.0	238.0	199.0	204.0	283.0	72.5	239	29.8
Pr	9.79	14.2	15.4	30.1	25.6	25.1	34.6	9.64	27.6	3.44
Nd	41.1	59.9	58.7	123.0	100.0	95.1	136.0	41.9	98.1	12.2
Sm	7.5	10.4	9.7	20.0	16.7	15.7	22.4	7.9	14.7	2.2
Eu	2.50	3.32	2.90	6.31	5.22	4.97	6.93	2.81	5.36	0.53
Gd	5.9	7.7	7.4	14.2	12.3	11.5	16.0	6.7	9.7	1.8
Tb	0.8	1.0	1.1	1.8	1.7	1.6	2.2	1.0	1.5	0.3
Dy	3.6	4.5	5.7	7.9	7.9	8.0	10.6	4.9	7.5	1.7
Ho	0.6	0.7	1.0	1.2	1.3	1.4	1.7	0.8	1.3	0.3
Er	1.4	1.7	2.9	2.8	3.4	3.7	4.6	2.3	3.6	0.9
Tm	0.17	0.18	0.39	0.29	0.39	0.43	0.54	0.29	0.45	0.13
Yb	1.0	1.2	2.6	1.9	2.5	2.9	3.6	1.9	3.1	0.9
Lu	0.14	0.16	0.37	0.25	0.31	0.39	0.47	0.27	0.41	0.14

(-) below detection limit; detection limit for Cr and Ni are 20 ppm.

Table 5: Nd and Sr isotopic compositions in samples from the Jasra alkaline-mafic-ultramafic complex.

Sm-Nd Compositions

S.No. ↓	Rock type	Sm (ppm)	Nd (ppm)	$^{147}Sm/^{144}Nd$	$^{143}Nd/^{144}Nd$ (2 sigma)	$^{143}Nd/^{144}Nd_{initial}$	ε_{Nd}
JS/5S	Ne Syenite	16.92	111.00	0.09221	0.512450±11	0.512387	-2.26
JS/15A	Ne Syenite	2.54	13.94	0.11030	0.512334±6	0.512258	-4.78
JS/22	Pyroxenite	49.73	346.60	0.08677	0.512487±6	0.512427	-1.48
JS/37	Pyroxenite	21.76	133.90	0.09828	0.512532±11	0.512464	-0.76
JS/34	Gabbro	8.68	45.18	0.11623	0.512397±17	0.512317	-3.63

Rb-Sr Compositions

S.No. ↓	Rock type	Rb (ppm)	Sr (ppm)	$^{87}Rb/^{86}Sr$	$^{87}Sr/^{86}Sr$ (2 sigma)	$^{87}Sr/^{86}Sr_{initial}$	ε_{Sr}
JS/5S	Ne Syenite	141.30	2087.0	0.19600	0.707949±10	0.707657	46.6
JS/15A	Ne Syenite	155.10	5320.0	0.08438	0.707060±10	0.706934	36.3
JS/22	Pyroxenite	8.31	960.8	0.03481	0.706575±10	0.706523	30.5
JS/37	Pyroxenite	39.49	2062.0	0.05542	0.706757±11	0.706674	32.6
JS/34	Gabbro	29.68	1248.0	0.06885	0.708994±13	0.708891	64.1

Initial Nd and Sr isotope ratios along with the epsilon values were calculated assuming an emplacement age of 105 Ma. Epsilon values are calculated using present-day ratios of $^{87}Sr/^{86}Sr$ = 0.7045 (DePaolo, 1988) and $^{87}Rb/^{86}Sr$ = 0.0827 (DePauolo, 1988) for Bulk Silicate Earth (BSE) and $^{143}Nd/^{144}Nd$ = 0.512638 (Goldstein et al., 1984) and $^{147}Sm/^{144}Nd$ = 0.1967 (Jacobsen and Wasserburg, 1980) for CHondritic Uniform Reservoir (CHUR). The internal precision for Sr and Nd isotope ratio measurement is ±0.0006 and ±0.0007, respectively, whereas, external precision for both the isotopes is ±0.0009. Two standards, La Jolla and BCR-1, were run with the Jasra samples for the measurement of $^{143}Nd/^{144}Nd$ ratios; measured values were 0.511854±7 and 0.512613±8, respectively. Similarly, NBS987 and NBS607 standards were run during $^{87}Sr/^{86}Sr$ analyses; measured values were 0.710239±10 and 1.20054±12, respectively.